FLIGHT VEHICLE DESIGN

Hyperbolic Paraboloid for a Ruled Preform of an X-Fitting: Calculation of Parameters

V. I. Khaliulin[a,*], V. V. Savitskii[b], A.V. Zhukov[b], and R. Sh. Gimadiev[c]

[a]*Tupolev Kazan National Research Technical University, ul. Karla Marksa 10, Kazan, 420111 Tatarstan, Russia*
[b]*Reshetnev AO ISS, ul. Lenina 52, Zheleznogorsk, 662972 Krasnoyarskii krai, Russia*
[c]*Kazan State Power Engineering University, ul. Krasnosel'skya 51, Kazan, 4200066 Tatarstan, Russia*
*e-mail: pla.kai@mail.ru

Abstract—A design and manufacturing process for composite fittings (a part of a truss structure of aircraft) is discussed. Intersecting tubular rods are connected via ruled surfaces such as a hyperbolic paraboloid. A mathematical model of X-fitting surface is developed, and numerical simulation of the fitting is performed to optimize its geometry. Due to the thing that interface surface is ruled, reasonable composite application and, as a result, high weight efficiency of the structure may be achieved.

INTRODUCTION

Truss, lattice and frame structures are applied in spacecraft structures [1–8] quite often. Their main elements are tubular rods and fittings connecting those rods. To achieve better weight efficiency, a transition from metals to composites takes place. Spacecraft structures should meet a set of requirements in strength, stiffness and thermal stability. These requirements are met by selection of components and a reinforcement pattern. In this case, selection of reinforcement patterns is a key to success in ensuring the aforementioned properties.

Reinforcement patterns for the tubular rods may be easily generated using the existing methods [9–11]. There is also a range of reliable processes for manufacturing of composite tubular rods [12–14].

Design of an optimum reinforcement pattern for fittings is a different issue. Normally, fittings are parts where two or more tubular rods intersect (Fig. 1).
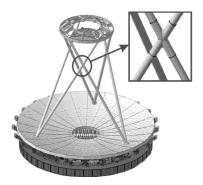

Fig. 1.

There is a wide range of fittings covered in the literature [15–21]. There are a few methods of manufacturing composite fittings, including lay-up [22–24], winding [25–27], and braiding [28–33]. Fittings, obtained using these methods, have irregular reinforcement patterns of the interface between tubular rods. This irregularity presents problems when performing design and strength computations, as it is very difficult to determine physical and mechanical properties of a part. It is also known that efficiency of composites depends significantly on the alignment of reinforcement pattern with applied forces. If they are not aligned, load-bearing capacity of a composite structure decreases. A composite structure, where all fibers are linear or have insignificant curvature, is considered to have the best reinforcement.

The aim of this study is to find the design and the process for fitting manufacturing that would provide the maximum weight efficiency due to reinforcement pattern. Reinforcement with maximum percentage of linear fibers in tubes intersection area is studied. To implement this idea, it is suggested to create surfaces in rods intersection area that would look like hyperbolic paraboloids. As is well known, a hyperbolic paraboloid is a ruled surface, i. e. it provides a possibility to design structures with linear reinforcement (Fig. 2) [34]. Presumably, it will provide weight decrease due to reasonable integration of reinforcement pattern.
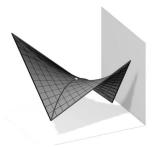

Fig. 2.

A set of issues has to be addressed to implement the idea of reinforcement along the surface of a hyperbolic paraboloid (or hypar):

—create reinforcement patterns to cover the saddle-shaped surface based on linear surfaces such as hypar;

—study the impact of bending radius on the weight efficiency of the X-fitting;

—develop a mathematical model of the interface between the saddle-shaped surface and tubular rods;

—develop a computer model of a fitting with hypar-type surfaces;

—study the impact of the parameters of a hypar on the evenness of the interface between the surface and the tubular rods;

—select optimum parameters of a hypar based on the requirements of minimum mass and even interface;

—develop a process of X-fitting manufacturing.

IMPACT OF X-FITTING INTERFACE RADII ON ITS LOAD-BEARING CAPACITY

Let us discuss a batch of ten fittings with different interface radii ranging from 3 to 38 mm (Fig. 3).

On one side, the ends of the tubes are embedded. On the other side, the ends are loaded with unit forces as shown in Fig. 3. The material is isotropic.

Finite element method is used to calculate equivalent stresses σ_{eq} in the interface. The analysis demonstrated that the mass of the fittings in the range of interface radii do not change significantly with deviation of around 1.5 %.
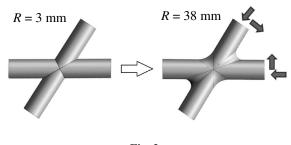
$R = 3$ mm $R = 38$ mm

Fig. 3.

Figure 4 presents the dependence of equivalent stresses on interface radii.
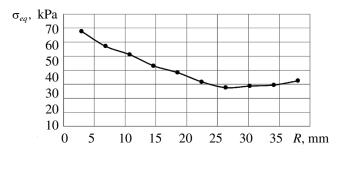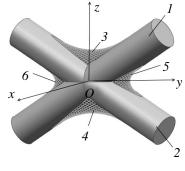

Fig. 4.

As seen in Fig. 4, as the radius increases, stresses decrease until a certain value is reached and then start to increase again. This dependence may be also considered for estimation of strength-to-weight ratio, because the mass of fittings changes insignificantly.

This calculation may be used to find the geometry of the saddle-shaped surface of a hypar as a first approximation.

A MATHEMATICAL MODEL OF AN X-FITTING

Equations for X-fitting definition

Geometrical model of an X-fitting is based on two cylinders *1*, *2* (Fig. 5) that interface with each other via hyperbolic paraboloids *3*, *4* and *5*, *6*.

Fig. 5.

The cylinders are identical. Generally, the structure has three planes of mirror symmetry. The origin $Oxyz$ is in the point where cylinders intersect. An angle between the Oz axis and the axes of cylinders is $\pm\alpha$. Equations of cylinders may be presented as follows

$$x^2 + (-y\cos\alpha + z\sin\alpha)^2 = r^2\,;\qquad(1)$$

$$x^2 + (y\cos\alpha + z\sin\alpha)^2 = r^2\,,\qquad(2)$$

where $0 \le \alpha \le \dfrac{\pi}{2}$; r is the radius of the cylinder, $r > 0$; x, y, z are the coordinate lines; α is an angle between the axis of the cylinder and the Oz axis.

Next step would be to place hyperbolic paraboloids on the newly formed crossing.

A hyperbolic paraboloid is a surface of the second order that is described by a canonical equation in Cartesian coordinates:

$$\frac{x^2}{a^2} - \frac{y^2}{b^2} = 2z\,,\qquad(3)$$

where a, b are the positive numbers; x, y, z are the variable coordinates.

The main feature of hypar—it is a set of straight lines (Fig. 2).

Let us describe the position of a hypar-type surface within the coordinate grid. It should be noted that hypars 3 and 4 as well as hypars 5 and 6 are located symmetrically to the Oxz, Oyz and Oxy, Oyz planes, respectively.

Figure 6a shows that sections of a hypar by the coordinate planes Oxz and Oyz are parabolas, and a section by the xyz plane is a hyperbola. In turn, the surface of hyperbolic paraboloid is obtained by moving the lower parabola so that its vertex slides along the upper parabola (Fig. 6b).
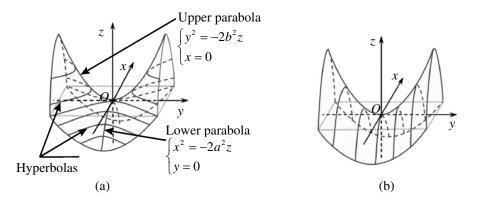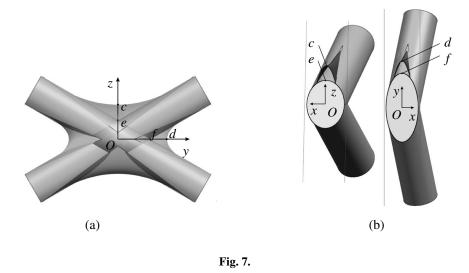

Fig. 6.

Let us transform the canonical equation into a more convenient form:

$$-Ax^2 + By^2 = z - c(d)\,,\qquad(4)$$

where $c(d)$ is the value that defines the coordinate of parabola vertices on the Oz (Oy) axis; it is selected randomly for a better fit onto the cylinders (Fig. 7).

In this case, in the section Oyz (where $x = 0$; A, B, $c > 0$), branches of parabola are directed upwards, and in the section Oxz (where $y = 0$; A, B, $c > 0$), branches of parabola are directed downwards (Fig. 5, hypar 3). Respectively, in the section Oyz, where $x = 0$; A, B, $d > 0$, and in the section Oxy, where $z = 0$; A, B, $d > 0$ (Fig. 7a, hypar 5).

(a)   (b)

Fig. 7.

The main limitation in generating the saddle-shaped surfaces is a condition of intersection or contact of parabolas with ellipses that appear where the Oxz or Oxy planes intersect with cylinders (Fig. 7b).

Here $c(d)$ are the vertices of a parabola; $e(f)$ is the intersection point of two cylinders with the Oz (Oy) axes . Let us find the factors A and B.

Positions of points e and f as intersections of two cylinders along the Oz and Oy axes, are determined by the following equations:

$$e = \frac{r}{\sin\alpha}; \ \ f = \frac{r}{\cos\alpha}.$$ (5)

Then parabolas that form hypars are built.

Let us review equations of hyperbolic paraboloids with the parameter c. The parameter c is located on the Oz axis and may be either positive or negative.

By transforming the canonical equation, we get the following equations, corresponding to hypars 3 and 4:

$$-\frac{c\sin\alpha + \sqrt{c^2\sin^2\alpha - r^2}}{2r^2\sin\alpha}x^2 + \frac{\cos^2\alpha}{4\sin\alpha(c\sin\alpha - r)}y^2 = k(z - c),$$ (6)

where $0 \le \alpha \le \dfrac{\pi}{2}$, $c > 0$, $r > 0$, $k = 1$, $k = -1$, respectively, for hypars 3 and 4.

In a similar way, for hypars 5 and 6 an equation with the parameter d is considered:

$$-\frac{d\cos\alpha + \sqrt{d^2\cos^2\alpha - r^2}}{2r^2\cos\alpha}x^2 + \frac{\sin^2\alpha}{4\cos\alpha(d\cos\alpha - r)}z^2 = k(y - d),$$ (7)

where $k = 1$ and $k = -1$, respectively, for hypars 5 and 6.

Finding the points of contact between a parabola and cylinders

When the hypar equation is found solving the following set of equations, one may find the coordinates of points M, M', N, N' (Fig. 8) of contact between a parabola and a cylinder on the Oyz plane:

—for hypar 3

$$\begin{cases} y_{con} = \pm\dfrac{\cot\alpha}{2B}; \\ z_{con} = \dfrac{\cot^2\alpha}{2B} + \dfrac{r}{\sin\alpha}; \end{cases} \tag{8}$$

—for hypar 5:

$$\begin{cases} y_{con} = \pm\dfrac{\tan\alpha}{2B}; \\ z_{con} = \dfrac{\tan^2\alpha}{2B} + \dfrac{r}{\cos\alpha}. \end{cases} \tag{9}$$

Based on Eqs. (6) and (7), we get $y = Bz^2 + c(d)$:

—for hypar *3*:

$$B = \frac{\cos^2\alpha}{4\sin\alpha(c\sin\alpha - r)};$$

—for hypar *5*:

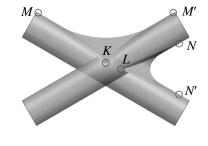$$\left(B = \frac{\sin^2\alpha}{4\cos\alpha(d\cos\alpha - r)} \right).$$

Fig. 8.

The next step is to find coordinates of contact points K, K', L, L' between parabolas and ellipses on the Oxz and Oxy planes by solving the following equations:

—for hypar *3*:

$$y = -Ax^2 + c, \quad x_{1,2} = \pm\frac{\sqrt{4r^2A^2\sin\alpha^2 - 1}}{2A\sin\alpha}, \tag{10}$$

where $A = \dfrac{c\sin\alpha + \sqrt{c^2\sin^2\alpha - r^2}}{2r^2\sin\alpha}$;

—for hypar 5:

$$y = -Ax^2 + d, \quad x_{1,2} = \pm\frac{\sqrt{4r^2A^2\cos\alpha^2 - 1}}{2A\cos\alpha}, \tag{11}$$

where $A = \dfrac{d\cos\alpha + \sqrt{d^2\cos^2\alpha - r^2}}{2r^2\cos\alpha}$.

SELECTION OF HYPAR PARAMETERS TO ENSURE INTERFACING WITH CYLINDERS

Let us review algorithms for building a hypar that interfaces with cylinders. To study the interface, let us perform a numerical experiment by building 3D models of X-fitting in Siemens NX software.

Let us set specific dimensions of the X-fitting: the radii of the cylinders will be $r = 50$ mm, the angle between the coordinate axis Oz and the cylinder axis is $\alpha = 60$ deg. Then equations of the cylinders will look as follows

$$x^2 + \left(-\frac{k}{2}y + \frac{\sqrt{3}}{2}z\right)^2 = 50^2,$$

where $k = -1$ for cylinder 1, $k = 1$ for cylinder 2.

Practically, there are two variants of building hypars that interface with cylinders:

—variant 1, when the guiding parabola is tangent to two generating lines of cylinders in the Oyz section, while the generating parabola intersects cylinders;

—variant 2, when the generating parabola is tangent to the cylinders in the Oxz plane, while the guiding parabola in the Oxz plane intersects cylinders.

Equations for hypars within the first and second variants are as follows:

—for hypar 3:

$$-\frac{c\frac{\sqrt{3}}{2} + \sqrt{c^2\left(\frac{\sqrt{3}}{2}\right)^2 - 50^2}}{m50^2\frac{\sqrt{3}}{2}}x^2 + \frac{\left(\frac{1}{2}\right)^2}{n\frac{\sqrt{3}}{2}\left(c\frac{\sqrt{3}}{2} - 50\right)}y^2 = z - c\ ; \tag{12}$$

—for hypar 5:

$$-\frac{d\frac{1}{2} + \sqrt{d^2\left(\frac{1}{2}\right)^2 - 50^2}}{t50^2\frac{1}{2}}x^2 + \frac{\left(\frac{\sqrt{3}}{2}\right)^2}{l\frac{1}{2}\left(d\frac{1}{2} - 50\right)}z^2 = y - d\ , \tag{13}$$

here for variant 1: $m = 1$, $n = 4$, $t = 1$, $l = 5$; for variant 2: $m = 2$, $n = 6$, $t = 2.5$, $l = 6$.

Setting parameters c and d and using Eqs. (12) and (13), it is possible to create different variants of hypars for cylinder interface.

STUDY OF INTERFACES BETWEEN A HYPAR AND CYLINDERS

A key in selecting the parameters of a hypar is to ensure as smooth interface with cylinders as possible. Variables are as follows: selection of one of the two variants of contact of guiding and generating parabolas, depth of the fit that is specified by the parameters c and d.

Saddles of a hypar that fit into the areas with the large and small interface radii of the cylinders are limited by straight lines (see Figs. 2 and 5), i. e. the projection of a hypar on a plane is a diamond. When the saddle is fitted, the boundary lines "cut" into the bodies of cylinders. The value of the cut-in is denoted as δ_n. Obviously, the optimum hypar will have the least values of δ.

To conduct the numerical experiment, let us create twelve X-fittings with identical cylinders. Six samples correspond to variant 1, where the guiding parabola contacts with the longitudinal generating lines of cylinders. The other six samples correspond to variant 2, where the generating parabola contacts with cylinders in the Oxz plane Three X-fittings with various parameters c and d are designed under variants 1 and 2. The parameter c takes the values 85, 98, 110, and the parameter d —120, 135, 150.

Then the line of guiding parabola is divided into seven even sections between the point of contact with the cylinder and Oxz plane of symmetry. A plane perpendicular to the axis of cylinder *2* passes through the origin of each section. Depth of saddle cut into the cylinder is determined in each of eight sections.

Let us consider an example corresponding to variant 2, i. e. when the hypar contacts with the ellipse generated by cylinders in the Oxz section while the guiding line cuts into the cylinder in the point G_1 and comes out in the point G_2 (Fig. 9).
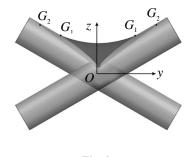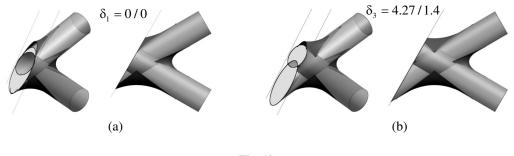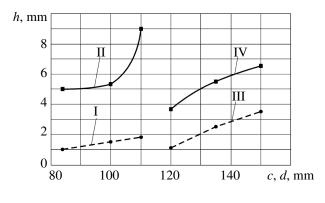

Fig. 9.

Saddle parameters are as follows: $c = 75$, $d = 135$. Figure 10 illustrates simulation of hypars *3* and *6* crossing the cylinders. Only two out of eight sections are demonstrated, namely, section 1 (Fig. 10a) and section 3 (Fig. 10b). Simulating all the possible saddle fits, it is possible to find the maximum cut-in for every one of three parameters c and d.

(a)   (b)

Fig. 10.

Curves I and II on graphs (Fig. 11) show the dependence between the maximum cut-in of hypar *3* and saddle fit parameter c for variants 1 and 2, respectively. The same is demonstrated for the cut-in of hypar 5 depending on the parameter d (curve III for variant 1 and curve IV for variant 2).

Fig. 11.

The graphs (see Fig. 11) show that maximum cut-in depth of hypars increases, when c and d increase. It is also seen that under variant 1 (dotted line) this depth is significantly less compared to variant 2 (solid line).

SELECTION OF A REASONABLE SADDLE SURFACE BASED ON INTERFACE

In designing X-fitting, it is obviously reasonable to select the one that has the better mechanical properties and minimum cutting into cylindrical elements. Under these conditions, reinforcement fibers have minimal bending in the interface between the hypar surface and a cylinder.

At the next stage, hypars are generated in the area of cylinder interface (Fig. 9). In any case, we will see saddle cutting into the cylinders. To prevent cutting of the hypar into the cylinders and building straight lines that generate the ruled surface of the hypar, surfaces of the cylinders are dissected by planes passing through the boundary lines of the hypar (Fig. 12a).

(a)   (b)

Fig. 12.

The next step would be generating straight lines of the hypar. To do that, straight lines are drawn through the point of contact between a hypar and a cylinder, where they intersect, and through the points of contact with parabolas of the cylinder. These straight lines are divided into a certain amount of sections, and straight lines are drawn through these points (Fig. 12b).

Different variants of rounding may be performed to provide smooth transition of fibers in the interfaces.

CONCLUSIONS

Fitting reinforcement pattern is suggested. The pattern provides a possibility to enhance its high weight efficiency. The main idea is to create an interface based on a ruled surface, such as a hyperbolic paraboloid, between crossing tubular rods.

Application of such a structure assumes creating a method of strength analysis of the fitting with hypar-based interfaces and a process to create a preform of the fitting in the future. A concept of hypar-type ruled surfaces may be spread on other aircraft structures as well, for example, fillets.

ACKNOWLEDGEMENTS

REFERENCES

1. Ermolaev, V.I. et al., *Sputnikovaia platforma "Ekspress-1000"* (Express-1000 Satellite Platform), Babuk, V.A. and Testoedov, N.A., Eds., St. Petersburg: Baltiiskii Gos. Tekhnicheskii Universitet, 2015.
2. Gvamichava, A.S. and Koshelev, V.A., *Stroitel'stvo v kosmose* (Space Engineering), Moscow: Znanie, 1984.

3. *Setchatye oboloshki – konstruktsii XXI veka* (Lattice Shells—the Structures of the XXI century), URL: https://territoryengineering.ru/bez-rubriki/setchatye-oboloshki-konstruktsii-xxi-veka.

4. Mikhailov, V.V. and Sergeev, M.S., *Prostranstvennye sterzhnevye konstruktsii pokrytii (struktury)* (3D Truss Structures of Coverages), Vladimir: Izd. VlGU, 2011.

5. Urmansov, F.F., Shchepalin, V.I., Voronin, A.A., and Denisov, A.V., RU Patent no. 2352024, *Byull. Izobret.*, 2009, no. 10.

6. Zimin, V.N. and Smerdov, A.A., Design of Composite Connecting Points for Optimization of Composite Multiple-Section Space Truss Structures, *Vestnik SibGAU*, 2017, vol. 18, no.1, pp. 123–131.

7. MacNeal, P.D. and Jewett, K.A., Design and Fabrication of a Large Primary Reflector Structure for Space Laser Power Beaming, *Proc. of OE/LASE,* Los Angeles, 1994, vol. 2121, p. 91.

8. Plathner, D., A 12 m Telescope for the MMA-LSA Project, URL: https://library.nrao.edu/public/memos/alma/main/memo259.pdf.

9. Dudchenko, A.A., Lur'e, S.A., Solyaev, Yu.O., Zhavoronok, S.I., Khaliulin, V.I., and Batrakov, V.V., Calculation, Design and Manufacturing Technology for a Thermally Stable Composite Rod, *Konstruktsii iz Kompozitsionnykh Materialov,* 2016, no. 1(141), pp. 3–11.

10. Samipour, S.A., Khaliulin, V.I., and Batrakov, V.V., A Method for Calculating the Parameters for Manufacturing Preforms Via Radial Braiding, *Journal of Machinery Manufacturing and Reliability*, 2017, vol. 46, no. 3, pp. 302–308.

11. Gainutdinov, V.G., Abdullin, I.N., and Musavy-Safavy, S.M., Calculation of Design Relative Density for Rational Sandwich Structure with Truss Core, *Izv. Vuz. Av. Tekhnika*, 2016, vol. 59, no. 1, pp. 59–63 [Russian Aeronautics (Engl. Transl.), vol. 59, no. 1, pp. 64–68].

12. Savitskii, V.V., Staritsyn, A.V., Batrakov, V.V., and Khaliulin, V.I., Design and Development of Truss Core for Spacecraft Sandwich Panel, *Naukoemkie Tekhnologii,* 2017, vol. 18, no. 12, pp. 59–65.

13. Khaliulin, V.I., Bezzametnova, D.M., and Gaifullin, B.R., Development of a Process for Manufacturing Composite Truss Cores for Sandwich Panels by Tailored Fiber Placement and Transfer Molding, *Vestnik Kazanskogo Gosudarstvennogo Tekhnicheskogo Universiteta im. A.N. Tupoleva,* 2015, vol. 71, no. 6, pp. 31–36.

14. Khaliulin, V.I., Khilov, P.A., and Toroptsova, D.M., Prospects of Applying the Tailored Fiber Placement (TFP) Technology for Manufacture of Composite Aircraft Parts, *Izv. Vuz. Av. Tekhnika*, 2015, vol. 58, no. 4, pp. 127–132 [Russian Aeronautics (Engl. Transl.), vol. 58, no. 4, pp. 495–500].

15. Chernov, S.A. and Chernyi, A.N., RU Patent no. 2623507, *Byull. Izobret.*, 2017, no. 18.

16. *Razrabotka konstruktsii i tekhnologii izgotovleniya uzlov sochleneniya trubchatykh elementov iz polimernykh kompozitsionnykh materialov* (Design and Development of the Process for Manufacturing of Articulations Between Polymer Composite Tubular Elements), URL: http://www.sktb-plastik.ru/176.

17. Carbon Fiber 0.5" Pultruded Tube Molded Connectors, URL: https://dragonplate.com/ Carbon-Fiber-05-Pultruded-Tube-Molded-Connectors.

18. Carbon Fiber Joint – 5 Way Pass through – Fits 2.00" OD Tubes, URL: https://www.rockwestcomposites.com/connector-accessories/cfj-5way-200.

19. Yang, X., Bai, Y., Luo, F.J., Zhao, X.-L., and He, X.-H., Fiber-Reinforced Polymer Composite Members with Adhesive Bonded Sleeve Joints for Space Frame Structures, *Journal of Materials in Civil Engineering,* 2017, vol. 29, no. 2, URL: https://ascelibrary.org/doi/10.1061/%28ASCE%29MT.1943-5533.0001737.

20. 3D Printing Nodes: "Space-Frame", URL: https://studiofathom.com/blog/space-frame-table-utilizes-3d-printed-nodes-for-complex-design.

21. *Fermennye konstruktsii iz kompozitsionnykh materialov* (Composite Truss Structures), URL: http://1000innovations.blogspot.com/2018/09/composite-truss-structures.html.

22. Vlasov, A.Yu., Obvertkin, I.V., and Martynov, V.A., RU Patent no. 2629487, *Byull. Izobret.*, 2017, no. 25.

23. Vlasov, A.Yu., Serzhantova, M.V., and Andreeva, Ya.A., Innovative Technology for Composite Part Manufacturing at SibGAU Resource Center "Spacecraft and Systems", *Issledovaniia Naukograda,* 2016, nos. 1–2 (16), pp. 8–12.

24. Fiberglass Tubing Supply, URL: https://www.fiberglasstubingsupply.com/services/flame-retardant-tubes.

25. Malkov, I.V., Scientific Principles of Winding CFRP Elements of Truss Structures for Spacecraft, *Cand. Sci. (Tech.) Dissertation*, Lugansk: Vostochnoukrainskii Nats. Univ., 2001, p. 36.

26. Dobrodushina, M.G., Kavun, V.V., Moskalev, S.I., and Shchudro, A.P., A Review of Thermally Stable Spacecraft Structures, *Kosmicheskaia Tekhnika. Raketnoe Vooruzhenie*, 2015, no. 2 (109), 2015, pp. 38–42.

27. Multiple Filament Winder. Proposal Based on Our Unique CFRP Molding Technology, URL: https://www.muratec.net/at/filamentwinder.html28.

28. Uozumi, T. and Kito, A., Carbon Fibre-Reinforced Plastic Truss Structures for Satellite Using Braiding / Resin Transfer Moulding Process, *Proc. of the Institution of Mechanical Engineers*, Part L: *Journal of Materials: Design and Applications*, 2007, vol. 221, pp. 93–101.

29. Uozumi, T., Kito, A., and Yamamoto, T., CFRP Using Braided Preforms / RTM Aircraft Application, *Advanced Composite Materials*, 2005, vol. 14, no. 4, pp. 365–383.

30. Uozumi, T. and Hirukawa, M., Braiding Technologies for Commercial Applications, *Proc. 6th Int. SAMPE Symposium & Exhibition*, Tokyo, 1999, pp. 497–500.

31. Kobayashi, H., Nakama, N., and Maekawa, Z., Fabrication and Mechanical Properties of Braided Composite Truss Joint, *Proc. 37th Int. SAMPE Symposium and Exhibition*, Anaheim, CA, 1992, A93-15726 04-23, pp. 1089–1103.

32. Uozumi, T., Recent Development of Muratec Braider, *Proc. 4th Int. Symposium of TEXCOMP*, Kyoto, 1998, pp. 9–10.

33. Azumi, Y., Tange, A., Nishiwaki, T., and Hamada, H., Design Method for Beam Members with Braided Composites, *Proc. 4th Int. Symposium of TEXCOMP*, Kyoto, 1998, p. 24–27.

34. Atanasyan, L.S. and Bazylev, V.T., *Geometriya* (Geometry), Moscow: Prosveshchenie, 1986, part 1, pp. 120–142.